International Journal of Pharmaceutics, 47 (1988) 141–155
Elsevier

IJP 01592

Frusemide crystal forms; solid state and physicochemical analyses

Chris Doherty * and Peter York

Department of Pharmaceutical Technology, Bradford University, Bradford, West Yorks (U.K.)

Received 31 March 1988)
(Accepted 14 April 1988)

Key words: Frusemide; Polymorph; Crystal properties; X-ray diffraction; Differential scanning calorimetry; Solid state NMR; Solubility; Dissolution; Molecular conformation

Summary

The diuretic frusemide has been reported to occur only in one crystal form (frusemide I). This work details the production and initial characterisation of a second crystal form (frusemide II). The formation of frusemide II was shown to be solvent dependent, being recrystallised by a solvent-evaporation process from methanol or ethanol and inhibited by the addition of water (5% v/v level). X-Ray powder diffraction patterns indicated differences in the crystal packing of the two forms whilst analysis of DSC thermograms defined changes in the melting/degradation event and a small endotherm, occurring only in frusemide I, 81°C below the melting endotherm. Infrared (IR) spectral changes included marked shifts corresponding to the sulphonamide N–H and S=O stretching vibrations suggesting the presence of an altered hydrogen bonding sequence in the frusemide II crystal. Solid state ^{13}C-CP/MAS analyses of frusemide I and II revealed marked differences in the chemical environments of specific carbon atoms reflecting a change in molecular conformation. In addition, a two component $T_{1\rho}$ relaxation time indicated domains within the frusemide II crystalline form possessing differing degrees of order or rigidity. The physicochemical consequences of the solid state changes in frusemide II include a 63% increase in aqueous equilibrium solubility and a 58% increase in the dissolution rate from constant surface area discs, relative to frusemide I.

Introduction

The solid state structure and physicochemical properties of a substance are dependent on the crystal form. When several molecular arrangements are possible and the crystal form is altered polymorphism is said to exist. Haleblian and McCrone (1969) conclude that almost every organic material can exist in different polymorphic states. The choice of a suitable drug polymorph can affect the stability and effectiveness of pharmaceutical formulations (e.g. physical stability, chemical stability, dissolution, solubility and clinical response). Several detailed reference works exist describing the characterisation of drug polymorphs (Carstensen, 1973; Burger and Ramberger, 1979a, b; York, 1983).

Many techniques are available to the pharmaceutical scientist to monitor and assess polymorphism including X-ray diffraction (Chrzanowski et al., 1984), thermal analysis (DSC, DTA TGA) (Miyata et al., 1985), infrared spectroscopy (IR) (Sekiguchi et al., 1980), optical microscopy with polarized light, electron microscopy, dilatometry, Raman spectroscopy (Bellows and Chen,

* *Present address*: Faculty of Pharmacy, University of Toronto, 19 Russell St., Toronto, Ont. M5S 1A1, Canada.

Correspondence: P. York, Department of Pharmaceutical Technology, Bradford University, Bradford, West Yorks, BD7 1DP, England.

1977; Bolton and Prasad, 1981), density (Burger and Ramberger, 1981), and the recent high resolution solid state nuclear magnetic resonance (SSNMR) (Ripmeester, 1980; Flippen-Anderson et al., 1983; Byrn et al., 1985). The improvement in the resolution of SSNMR spectra obtained by proton decoupling, cross-polarisation (CP) and magic angle spinning (MAS) now enable more specific information to be gained concerning molecular conformations and interactions in powder samples.

NMR relaxation studies can also provide useful information on molecular motion in the solid state. Homogeneous pure-phase systems will exhibit a single magnetisation exponential decay while systems that display heterogeneity, e.g. samples that contain crystalline and non-crystalline domains, may exhibit more than one relaxation time constant (Fyfe, 1983). The proton relaxation time constants measured in this work, T_1 and $T_{1\rho}$, reflect spin lattice relaxation processes occurring in the MHz and kHz frequency ranges, respectively.

The drug examined in this work, frusemide, is a commonly prescribed diuretic agent. Frusemide is not reported to exhibit polymorphism and the single crystal X-ray structure has been determined (Lamotte et al., 1978). The synthesis and preparation of frusemide is the subject of a number of patents. In the context of the current work the final recrystallising solvent is of interest. In a British patent (Christensen, 1969) 70% ethanol was used, in an American patent (Yellin et al., 1973) 95% ethanol, and in a German patent (Christensen, 1967) "ethanol" was specified. Ethanol–water mixtures are assumed to be implied in the British and American patents.

The current work examines the solid state characteristics of frusemide samples recrystallised from a series of *n*-alcohols containing different levels of added water, with the aim of examining changes in hydrogen bond interaction and molecular conformation.

Materials and Methods

Frusemide BP ($C_{12}H_{11}ClN_2O_5S$; 4-chloro-*N*-furfuryl-5-sulphamoyl-anthranilic acid, also termed furosemide) (lot 309277) was obtained from APS Pharmaceuticals, Cleckheaton, U.K., frusemide standard from Hoechst Pharmaceuticals, U.K. (lot 170C879) and frusemide USP reference material from USPC, Rockville, U.S.A. Methanol (HPLC grade, Rathburn Chemicals, Scotland), ethanol (99.86% minimum, James Burrough, London) and *n*-propanol (> 99%, BDH, Poole) were used as recrystallisation solvents. All water used was double-distilled and deionised. All other reagents were of Analar grade unless stated.

Thermal analysis

Differential scanning calorimetry (DSC) thermograms were acquired using a Dupont 910 DSC and 1090 thermal analyser, calibrated with indium metal (99.9% purity, Dupont, melting point 156.6 °C, enthalpy of fusion 28.44 J/g). Samples (6–7 mg) were scanned at a rate of 10 °C/min at least in duplicate (40–270 °C). Thermogravimetric analysis (TGA) utilised a Dupont 951 TGA unit, 10–20 mg sample size and a scan speed of 10 °C/min (40–270 °C).

X-Ray powder diffraction

X-Ray powder diffraction (XPD) data were collected using a Philips PW 1200/00 generator (20 mA, 30 kV with copper-potassium-α radiation). Samples were scanned between 4–40° 2θ at a speed of 2° 2θ/min.

Hot stage microscopy

Physical changes in the samples on heating were monitored by hot stage microscopy (HSM) with a Stanton Redcroft Hot Stage Unit and Universal Temperature Programmer, heated at a controlled rate of 10 °C/min.

Infrared spectroscopy

Dispersive infrared (IR) analyses utilising potassium bromide discs, mineral oil mulls and rock salt solution cells (0.1 mm path length), involved multiscanning with a Perkin Elmer PE681 spectrometer. Variable temperature Fourier Transform infrared (VT-FTIR) spectra were recorded on a Mattson Sirius 100 spectrometer (2 cm^{-1} resolution), the samples being mounted in a Specac 21000 variable temperature cell. VT-FTIR spectra

were obtained in the following sequence; ambient temperature, 120 °C, 150 °C, and again at 120 °C during cooling. This sequence allowed correlations to be made between DSC and IR data on heating the frusemide samples.

NMR spectroscopy

Solution ^{1}H-NMR spectra were obtained at 250 MHz (Bruker Cryospec WM 250) from Fourier Transformations of 200 scans at 298K. An 80% v/v acetonitrile (99.5%D, Nuclear Magnetic Resonance, Bucks, U.K.): 20% v/v dimethylsulphoxide (99.8%D, CEA, France) co-solvent was used. Tetramethylsilane (TMS) was included as a reference. [^{13}C]Solution spectra were obtained on the same spectrometer using a 5 mm dual probe (^{1}H/^{13}C) at 62.89 MHz. Deuterated acetonitrile (CD_3CN) was used as a model non-polar solvent for frusemide at a concentration of 0.018 M.

^{13}C-solid state NMR spectra were obtained on a home-built double-resonance spectrometer (UEA 200, University of East Anglia, U.K., details of which can be found in Kenwright, 1986), utilising an Oxford Instruments superconducting magnet at 4.7 Tesla (^{13}C = 50.29 MHz). Spectrometer operation was controlled by custom-written software using a Nicolet NIC 1180 computer. Spectra were observed using magic angle spinning, cross-polarisation and proton-decoupling procedures. Solid state proton relaxation times (T_1-spin lattice and $T_{1\rho}$-spin lattice relaxation in the rotating frame) were obtained on a Magnion single channel, high power, pulse spectrometer.

HPLC assay

The frusemide content in the recrystallised samples was determined by HPLC using a Pye Unicam LC-XPD pump, a column packed with partisil 10 μm-ODS, a Pye Unicam LC-UV detector (272 nm), a mobile phase consisting of 35% v/v acetonitrile : 65% v/v orthophosphoric acid (0.0157 M) and a frusemide injection concentration of 8 mg/100 ml. Frusemide was well separated from the primary degradation product 2-amino-4-chloro-5-sulphamoyl anthranilic acid (saluamine). Estimation of the saluamine content was achieved using the same experimental conditions and injecting at a frusemide concentration of 50 mg/100 ml. Linear calibration curves were determined for each chemical entity.

Water content

The water content of the samples was analysed by gas liquid chromatography (GLC). 200 mg of each sample was dissolved in 2 ml of Karl Fisher grade methanol containing 10% v/v triethylamine and injected in duplicate onto a Porapak-Q column at 90 °C with an injection port temperature of 100 °C and thermal conductivity detector at 200 °C.

Equilibrium dissolution

Dissolution studies involved a discriminating constant surface area disc method (Doherty and York, 1987a) with a pH 4.95 sodium acetate-acetic acid buffer as the dissolution medium. Frusemide dissolution at 37 °C was monitored by an automated diode array spectrophotometer (272 nm) (Hewlett Packard HP8451A) for 60 min, each sample at least in duplicate. A diffusion-controlled dissolution process was assumed and the Noyes-Whitney equation applied with sink conditions prevailing;

$$dm/dt = k \cdot A \cdot S$$

where the measured dissolution rate, dm/dt, is calculated from the slope of the linear mass-dissolved/time plot (units of $\mu g \cdot min^{-1}$), k is the intrinsic dissolution rate constant, A is the surface area of the solid or the area of the diffusion layer and S is the concentration of solute at the solid/liquid interface.

Production of samples

A solvent evaporation-recrystallisation process was used, with methanol, ethanol and *n*-propanol as the recrystallising solvents. A study was made of the solid state effects of adding water (5–20% v/v) to the recrystallising solvents. 2 g of 'as received' frusemide was dissolved in 400 ml of the solvent or water co-solvent at 60 °C and evaporated to dryness in a vacuum oven (Gallenkamp OVL570, 60 °C, 1.5×10^3 Pa). Recovered solids were ground, sieved (90–250 μm fraction retained) and stored over molecular seive 5A for

48 h to complete the drying process. The size reduction process was not found to affect the crystal form.

It was found that a new crystal form of the drug (termed frusemide II) was recrystallised from methanol and ethanol while the addition of water (5–20% v/v) to these solvents resulted in the production of the original crystal form. In addition, it was found that the new crystal structure was formed preferentially during the initial drying period and located on the sides of the evaporating dish, while the original frusemide structure was formed in the bottom of the dish. During the initial drying period evaporation of solvent results in recrystallisation of frusemide at the edge of the dish and this is likely to involve a high rate of recrystallisation. Subsequently, as more solvent is removed, the drug will reach the solubility limit and recrystallise from solution. The difference in the kinetics of recrystallisation for these two situations may account for the formation of differing frusemide crystal forms. In this work the original crystal form is termed frusemide I and samples that were recrystallised from methanol or ethanol and harvested from the sides of the evaporating dish are termed frusemide II.

Results and Discussion

Differential scanning calorimetry (DSC)

The DSC thermograms for untreated frusemide, frusemide standard and reference materials show two endotherms (Fig. 1). The first endotherm was present in the range 136–139 °C and was not followed by any exothermic event. The melting endotherm, accompanied by degradation, occurred in the range 217–222 °C (Table 1). This melting temperature is higher than that recorded by the capillary tube method for the same material (203–206 °C). Although the first endotherm has been shown to be present in a literature DTA thermogram (Shin, 1979), no information concerning the nature of the endothermic process is currently available.

DSC data for the frusemide samples recrystallised from each solvent system studied are shown in Table 1. Recrystallisation of frusemide from methanol resulted in a lowering of the degradation temperature, preventing melting before degradation. The first endotherm was not found in frusemide samples produced from methanol or ethanol, but was present in samples recrystallised from propanol and all water co-solvent mixtures.

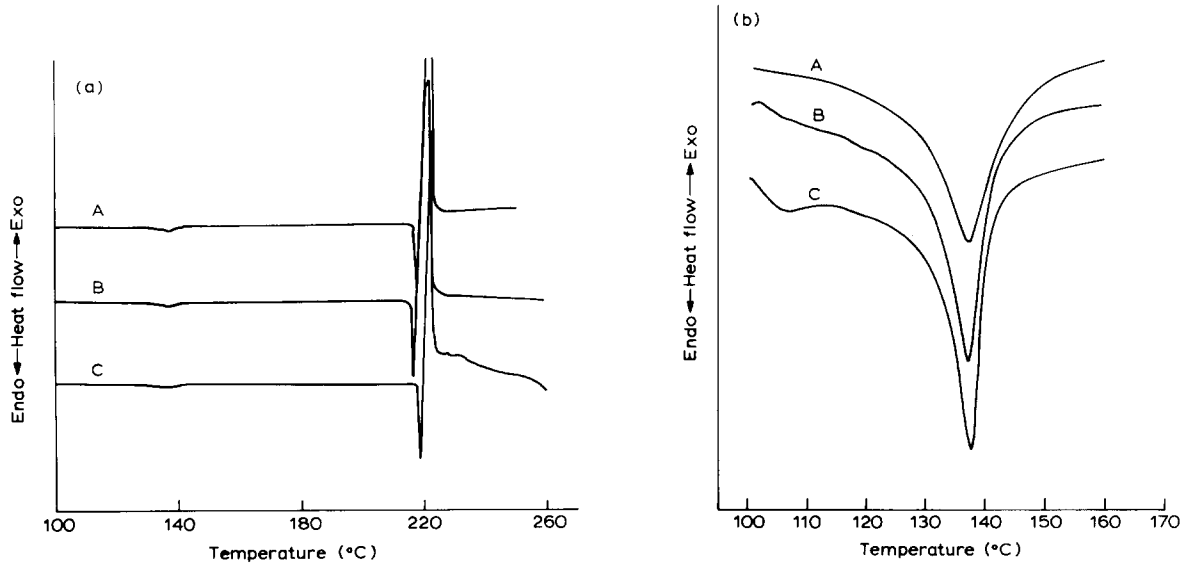

Fig. 1. DSC thermograms of untreated frusemide samples to show the melting endotherm and degradation exotherm (a) and an expanded plot to show the first endotherm (b) for commercial frusemide (A), standard frusemide (B) and reference frusemide (C).

TABLE 1

DSC peak temperatures for the first endotherm, melting endotherm and degradation exotherm in untreated and recrystallised frusemide thermograms

Figures represent the range of the data.

Recrystallising solvent/sample	No. of runs	Temperature (°C)		
		First endotherm	Melting endotherm	Degradation exotherm
Untreated group				
Frusemide BP	17	137–139	217–222	219–227
Standard frusemide	3	137–139	216–221	221–227
Reference frusemide	2	137	219–220	221–224
Recrystallised group				
Methanol *	7	ND	ND	210–216
95 : 5 methanol : water	8	136–139	207–212	213–220
90 : 10 methanol : water	4	135–137	208–211	212–217
80 : 20 methanol : water	6	136–139	210–213	215–220
Ethanol *	6	ND	210–216	214–222
95 : 5 ethanol : water	2	136–137	213–215	218–224
n-Propanol	4	134–137	215–216	219–225
95 : 5 *n*-propanol : water	2	136	213	217–218

ND = not detectible.

* Harvested from the side of the dish.

Addition of water to the solvent also resulted in a small increase in the degradation exotherm temperature allowing, for example, melting to occur before degradation in the frusemide sample recrystallised from 95% methanol : 5% water. These changes indicate the water level in the recrystallisation medium can influence the resulting crystal form, and by the observed changes on the degradation temperature, the lattice stability to a thermal stress.

The effect of changes in the solvent composition on the first DSC endotherm observed in frusemide I thermograms was quite marked and attempts were made to define the endothermic process that occurred over the 136–139 °C range. The endotherm was found to be reversible by re-heating a frusemide I sample that had been previously heated past the first endotherm temperature but to below the melting point, and then cooled. The area of the endotherm was not found to be altered (first run $\Delta H = 2.2$ kJ/mol, reheat $\Delta H = 2.1$ kJ/mol). In a similar way, reheating a cooled frusemide II sample did not result in any change in the thermogram. This would suggest that the two crystal forms are not interchangeable on heating, within the limits of the experiment.

In a study of the polymorphic forms of bromodiethylacetylurea (Doi et al., 1985), a comparable solid–solid transition was shown to have an endothermic energy change of $\Delta H = 3.14$ kJ/mol and this was attributed to the destruction of intermolecular hydrogen bonds, a change in molecular conformation and a reformation of an altered hydrogen bond network. This transition endotherm value is close to that observed in the DSC thermogram of frusemide I at 136–139 °C. From this data one hypothesis is that a crystal re-packing occurs in frusemide I at 136–139 °C. In frusemide samples not exhibiting the first endotherm (e.g. frusemide II), the crystal form may possess a different molecular conformation or hydrogen bonding sequence such that a disruption of the crystal packing does not occur.

Hot stage microscopy (HSM)

To further define the characteristics associated with the first endotherm in the frusemide I thermogram, samples of untreated and recrystallised

frusemide I (95% methanol : 5% water co-solvent) were heated to 150 °C. The crystals were seen to exhibit an abrupt physical change resulting in the break up of the crystals in the temperature range 135–140 °C. This was seen in many repeated samples, most notably with thin needle-like crystals. No melting was seen within the crystals immediately prior to, or during, the change. This

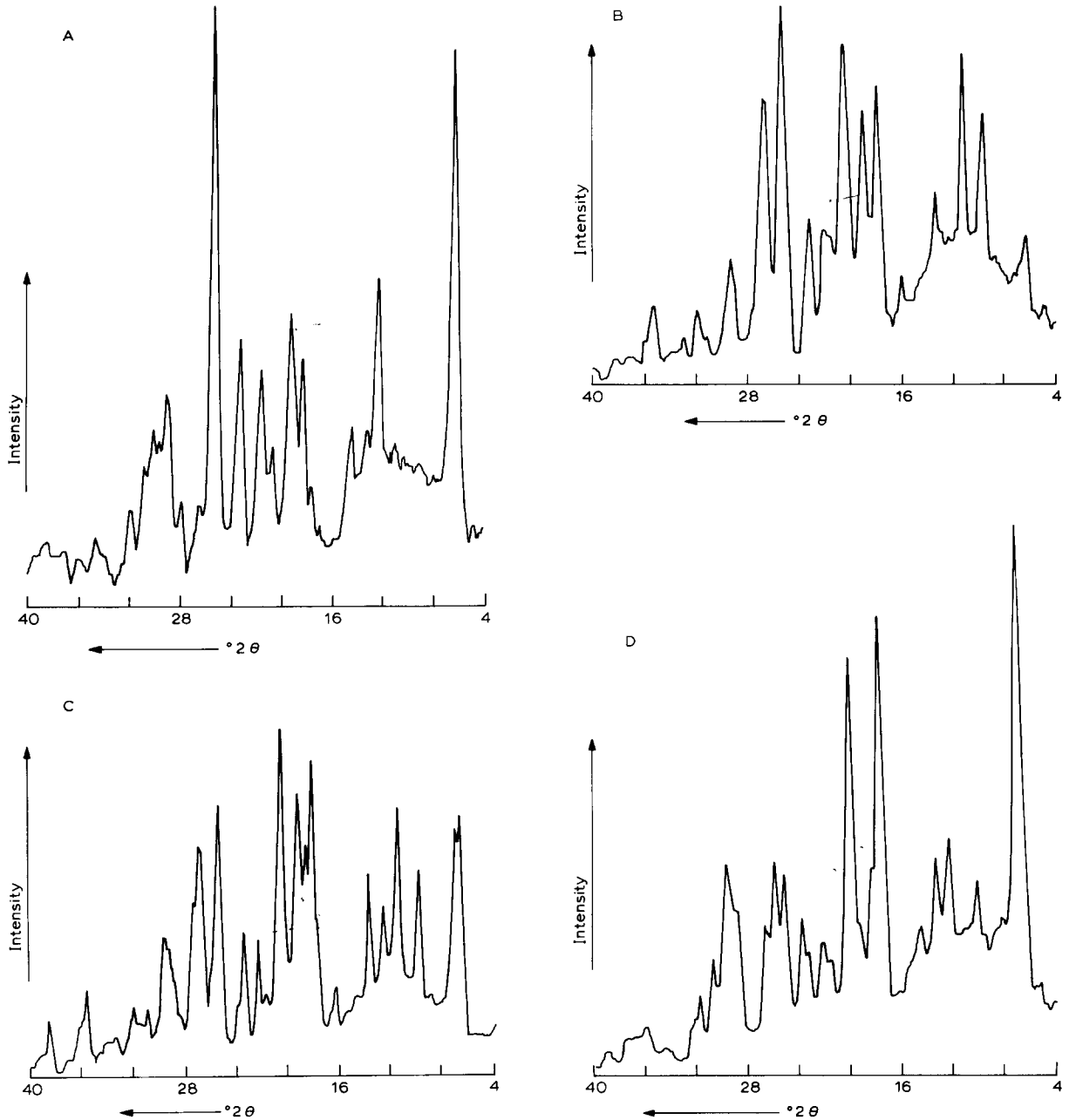

Fig. 2. XPD spectra for untreated commercial frusemide (A) and frusemide samples recrystallised from methanol (B), ethanol (C) and *n*-propanol (D).

physical change is an indicator of a solid state transformation, possibly involving an alteration in the crystal packing, corresponding to the DSC endotherm occurring at the same temperature.

Thermogravimetric analysis (TGA)

Untreated and recrystallised frusemide samples were examined by TGA using the procedure outlined above. No weight loss was recorded in any sample until 206–220 °C corresponding to the decomposition on melting seen in DSC thermograms. The data indicate that the solid state changes observed for frusemide II cannot be attributed to solvate formation. In addition, no weight loss was seen in the range 136–139 °C indicating that the endothermic event occurring at this temperature, observed in the frusemide I DSC thermogram, is not associated with any detectible weight loss.

X-ray powder diffraction (XPD)

XPD spectra were obtained for all frusemide samples for diffraction angles in the range 4–40° 2θ. The data for untreated and standard frusemide samples correlated with published XPD spectra for frusemide (DeCamp, 1984). The XPD spectra of samples recrystallised from methanol, ethanol or propanol differed significantly from that of the untreated frusemide (Fig. 2) with new diffraction lines being shown and alterations in the relative peak heights of other peaks. Adding water (5–20% v/v) to each recrystallising solvent resulted in samples displaying the original frusemide XPD spectrum, with only small differences in relative peak height. These minor effects may result from changes in crystal morphology and preferred orientation characteristics. The XPD changes observed for methanol and ethanol recrystallised samples, although not identical, displayed similar patterns while the propanol recrystallised frusemide sample exhibited another pattern.

The altered XPD patterns reflect a change in crystal packing and structure when frusemide is recrystallised from the solvents without added water, correlating with changes seen in DSC thermograms. The methanol and ethanol recrystallised samples were found to display similar DSC and XPD characteristics reflecting basic similarities in their crystal forms.

Infrared (IR)

The KBr disc spectrum of frusemide I agreed with reported spectra (Clark, 1969) and corresponds to the molecular structure shown in Scheme 1:

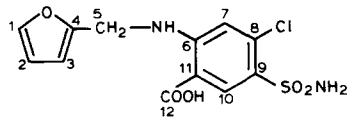

Scheme 1. Frusemide (4-chloro-*N*-furfuryl-5-sulphamoylanthranilic acid).

Frusemide I mull and KBr disc spectra were identical and a spectral assignment of principal functional group vibrations was made using spectra of similar structures (Pouchert, 1970). Dispersive IR spectra for frusemide samples recrystallised from methanol and ethanol (frusemide II) revealed pronounced shifts from the respective positions in the frusemide I spectrum (Fig. 3). Propanol recrystallised samples exhibited IR spectra identical to those for frusemide I, indicating that the altered XPD spectra for these samples were not associated with changes at the molecular level.

The addition of water to the methanol and ethanol solvents at the 5% v/v level resulted in frusemide samples exhibiting characteristic frusemide I spectra (Table 2). An IR mull spectrum of frusemide II agreed with the KBr disc spectrum indicating that the grinding and compaction processes involved in the production of KBr discs did not invoke IR spectral changes.

Solution IR spectra for frusemide I and II, utilising 1,4-dioxan as a solvent (0.033 M, 20 °C), were identical, demonstrating that the observed KBr disc spectral changes correspond only to a change in solid state interactions for the two crystal forms and that solution conformations are equivalent.

Many peaks in the frusemide II IR spectrum exhibited marked differences from the respective positions in the frusemide I spectrum. These were especially noticable in the 3200–3400 cm^{-1},

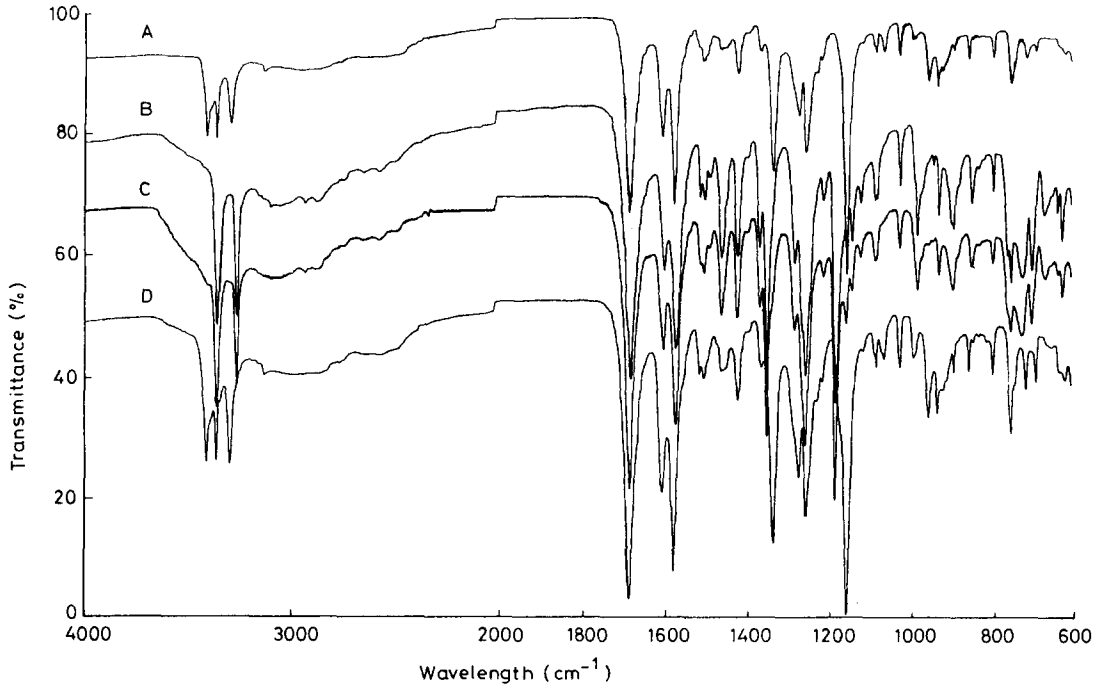

Fig. 3. Dispersive IR spectra (KBr disc) for untreated frusemide (A) and frusemide samples recrystallised from methanol (B), ethanol (C) and *n*-propanol (D).

TABLE 2

Dispersive IR spectral positions and suggested assignment for principal functional group vibrations in untreated and recrystallised frusemide samples

Sample	Wavenumber (cm^{-1})							
	N–H (S) [a]	N–H (S) [b]	N–H (S) [a]	C=O	N–H (B)	N–H (B)	S=O (ASY)	S=O (SYM)
Untreated group								
Frusemide BP	3402	3354	3289	1674	1595	1567	1327	1145
Standard frusemide	3402	3354	3288	1675	1595	1567	1326	1146
Reference frusemide	3402	3354	3288	1675	1596	1566	1327	1146
Recrystallised group								
Methanol	NF	3351	3257	1673	1592	1563	1342	1174
95 : 5 methanol:water	3403	3355	3289	1676	1597	1567	1328	1147
Ethanol	NF	3352	3257	1674	1593	1563	1342	1175
95 : 5 ethanol:water	3402	3354	3289	1676	1597	1567	1327	1146
n-Propanol	3403	3355	3290	1675	1596	1568	1326	1146
95 : 5 *n*-propanol : water	3403	3355	3289	1676	1597	1567	1328	1146

ASY = asymmetric S=O stretch; B = N–H bending vibration; NF = not found in spectrum; S = N–H stretch vibration; SYM = symmetric S=O stretch.

[a] Sulphonamide N–H vibration.

[b] Secondary amine N–H vibration.

1145–1350 cm^{-1} and 600–1000 cm^{-1} regions. Using the spectral assignment, the major shifts can be related to changes occurring in specific areas of the frusemide molecule and molecular conformation. In the 3200–3400 cm^{-1} region the secondary amine N–H stretching vibration is unaltered (3352 cm^{-1}). This would concur with published single crystal X-ray data for frusemide I (Lamotte et al., 1978) which demonstrated that the secondary amine proton was intramolecularly bonded to the adjacent carbonyl group, described and supported by proton NMR data in a previous report (Doherty and York, 1987b). An IR spectrum corresponding to the published crystal structure was provided (Dupont, 1985) and agreed with the frusemide I spectrum reported in this work. In frusemide II the intramolecular hydrogen bond remains and the carbonyl vibration is seen at 1674 cm^{-1} supporting this hypothesis. The two sulphonamide N–H stretching vibrations are shifted to lower wave number positions, the peak originally at 3402 cm^{-1} in the frusemide I spectrum being obscured by the secondary amine peak in frusemide II. The changes observed for the sulphonamide N–H stretching vibrations are also reflected in the S=O vibrations at 1145 cm^{-1} (symmetric stretch) and 1327 cm^{-1} (asymmetric stretch). These vibrations were found to shift by 29 and 15 cm^{-1}, respectively, to higher wave numbers. No significant changes in N–H bending vibrations were observed in any spectra.

The frusemide I crystal unit cell was shown to possess an intermolecular hydrogen bond network involving the sulphonamide groups (Doherty and York, 1987b). IR data for the frusemide II crystalline form revealed a change in the vibrations associated with the sulphonamide group and this suggests that there is an alteration in the hydrogen bond sequence within the crystal. This may result from a change in molecular conformation and crystal packing.

It may be suggested that the first endotherm seen in the DSC thermogram of frusemide I is a solid–solid transition for the transformation of frusemide I to frusemide II. Such a transition would result in marked IR changes above the temperature of the endotherm. To examine this hypothesis a variable temperature FTIR (VT-FTIR) study was conducted, spectra being recorded in the sequence; ambient temperature, 120 °C, 150 °C and 120 °C during cooling. The final spectra at 120 °C was incorporated in order to assess the reversibility of any changes resulting from heating past the temperature at which the first DSC endotherm occurs. A similar study was made of frusemide II for comparison.

Examination of the VT-FTIR spectra for frusemide I (Fig. 4A) revealed no significant shifts in the positions of the principal functional group vibrations. The endothermic process observed in the DSC thermogram of frusemide I is therefore not reflecting a frusemide I–frusemide II transformation. The proposed interpretation of the endothermic process at 136–139 °C in frusemide I is a subtle change in molecular conformation and crystal packing. The VT-FTIR spectrum recorded above the first endotherm temperature in frusemide I suggests that the hydrogen bonding sequence is of a similar nature to that below the endotherm temperature.

The VT-FTIR spectra of frusemide II (Fig. 4B) show no significant changes in the positions of the principal functional group vibrations on heating to 150 °C. Several minor effects were observed and these included an increase in the intensity of a small peak at 3407 cm^{-1} and a change in the peak splitting patterns below 1150 cm^{-1}. The frusemide II IR shifts observed at room temperature were still apparent after heating to 150 °C indicating the thermal stability of frusemide II under the test conditions.

The data suggest that frusemide I and II are discrete crystal structures of frusemide and that they do not transform on heating to 150 °C, within the experimental conditions examined.

Nuclear magnetic resonance (NMR)

The ^{1}H-solution NMR spectra of frusemide I and II in an 80 : 20% v/v acetonitrile : dimethylsulphoxide solvent were identical. This confirms the observation from IR spectra that the two samples exhibit equivalent conformations in solution and that only one chemical species is present.

The ^{13}C-CP/MAS solid state NMR spectra of frusemide I and II (Fig. 5) show significant chemical shift differences for specific carbon atoms

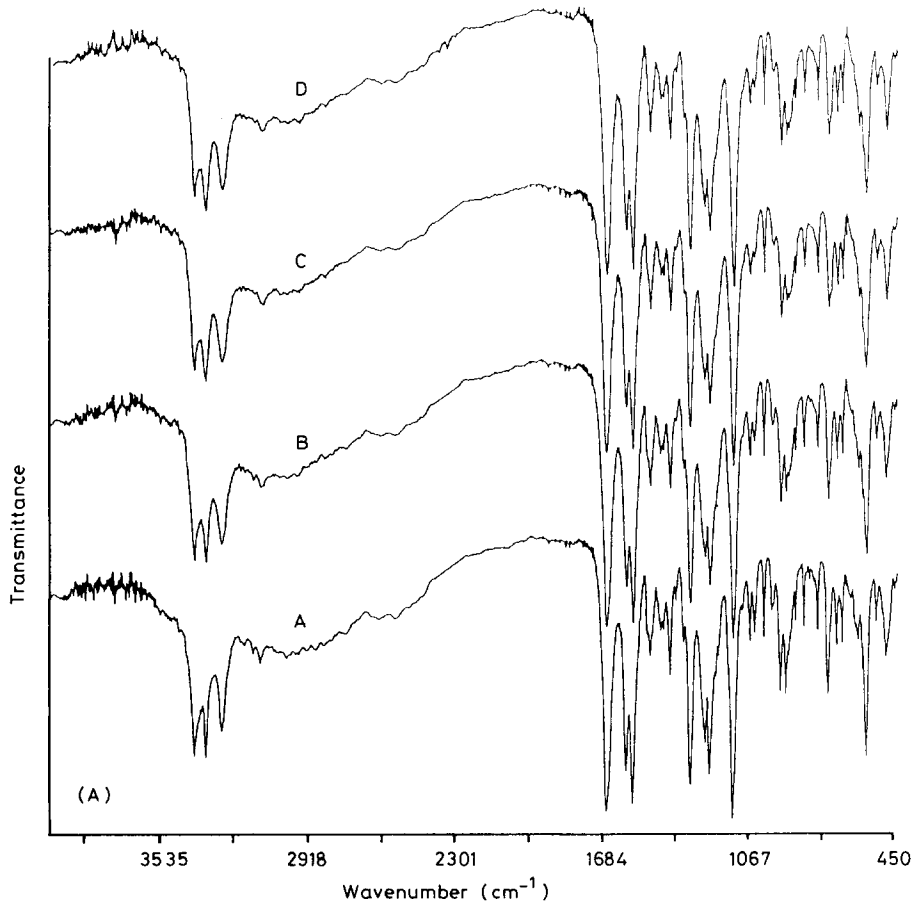

Fig. 4. Variable temperature FTIR spectra for frusemide I (a) and frusemide II (b) recorded in the sequence: (A) ambient temperature, (B) 120 °C, (C) 150 °C and (D) 120 °C on cooling.

(Table 2). In some cases a peak could not be accurately assigned and therefore two possible peaks are given for these carbons in the Table 3. The data for frusemide II indicate a splitting of the carbonyl carbon resonance, C_{12}, and also that of C_1 in the furan ring. This splitting pattern is indicative of two chemical environments producing differing levels of deshielding. The presence of two dissimilar molecular conformations or asymmetric units in the frusemide II unit cell may account for these patterns.

One of the peaks assigned to either C_7 or C_{10} (in the benzene ring) has shifted considerably from the position of 116.6 ppm in frusemide I. There is a peak at 51.0 ppm in frusemide II which is very close to the solution chemical shift for methanol. However, no evidence was found to indicate the presence of methanol in the solution spectrum and this peak could also represent a spinning side band. The observed shifts in the frusemide II spectrum involve marked changes in the chemical environments of C_1, C_7 or C_{10} and C_{12} and to a lesser extent C_5 and C_8. In addition several peak intensity differences are evident between the spectra of frusemide I and II, notably for C_6, C_9, C_{11} and C_{12}. The peak intensity is related to the relaxation characteristics of the atom and, in the case of ^{13}C-nuclei, the principal mechanism is spin–spin relaxation (T_2). The spectra indicate that the T_2 relaxation time constant is markedly longer for several of the carbon atoms in frusemide II.

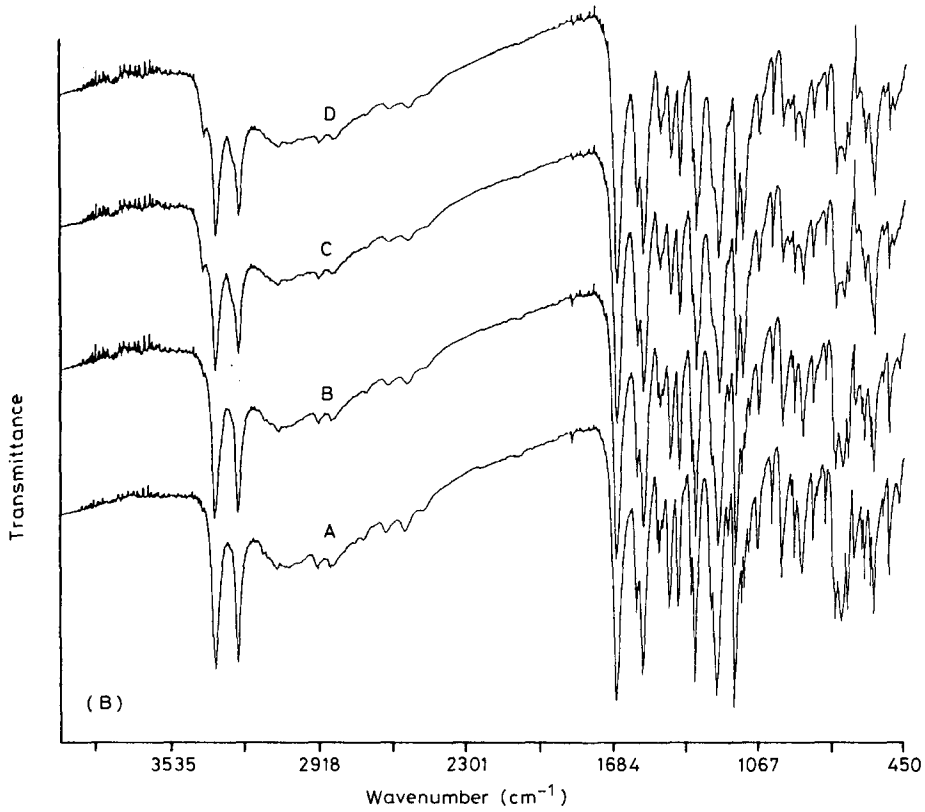

Fig. 4 (continued).

The ^{13}C-SSNMR data suggest a change in the molecular conformation of the frusemide molecule in the crystal form II. This may be associated with an altered hydrogen bonding sequence and a different crystal packing arrangement, concurring with IR and XPD data.

The comparison of the ^{13}C-chemical shifts for frusemide in solution and solid states is shown in Table 3. Both frusemide I and II solid state spectra exhibit marked shifts from the relative position in the solution spectrum, with both upfield and downfield shifts evident. These chemical shift changes are of a similar order of magnitude to those reported to occur between the solution and solid state ^{13}C-spectra of glyburide where conformation changes are inferred (Byrn et al., 1986). The data suggest that the solution conformation of frusemide is different from that present in either of the two solid state crystal forms when employing a relatively non-polar solvent.

Analysis of the solid state proton relaxation times T_1 and $T_{1\rho}$ also reveal differences between frusemide I and II (Table 4). The T_1 values, reflecting relaxation in the MHz range, are quite similar for the two crystal forms. However values for relaxation in the kHz range, $T_{1\rho}$, differ and the frusemide II sample can be described as a two-component system. The shorter $T_{1\rho}$ in frusemide II is attributed to a more mobile, less ordered phase present within a more highly ordered and rigid system, possibly resulting from a partial or regional disruption of the crystal lattice. The $T_{1\rho}$ value for frusemide I represents a more uniformly rigid system and this correlates with the crystalline material seen in the XPD spectrum. Short $T_{1\rho}$ values are often seen in relaxation studies of

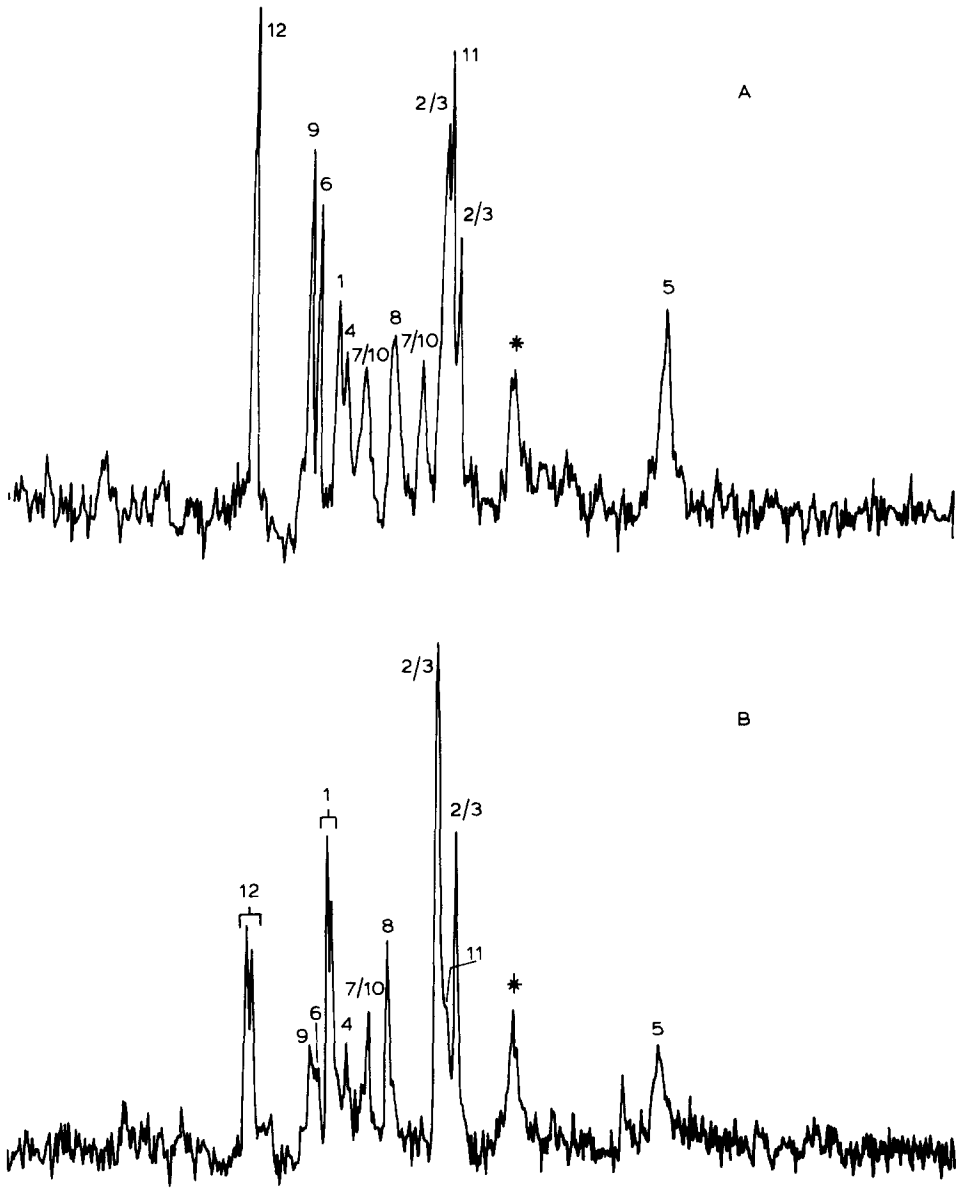

Fig. 5. ^{13}C-CP/MAS solid state NMR spectra for frusemide I (A) and frusemide II (B) at ambient temperature. The peaks marked with a star are due to the delrin rotor base. Numbered peaks refer to the carbon assignments in Table 3.

semi-crystalline and amorphous polymers and describe the highly mobile elements (Havens and Koenig, 1983).

Chemical analyses

Analysis of the main chemical component in the frusemide samples by HPLC revealed no discernible purity difference between any sample or crystal form (> 99% w/w purity). Analysis of the primary degradation product saluamine by HPLC also revealed no significant difference between untreated and recrystallised frusemide samples (0.06–0.08% w/w saluamine content).

The water content of untreated and recrystal-

TABLE 3

Comparison of ^{13}C-solution chemical shifts for frusemide in deuterated acetonitrile (CD_3CN, 0.018 M, ambient temperature) and ^{13}C-CP/MAS solid state shifts for frusemide I and II, with suggested assignments

All chemical shifts are relative to tetramethylsilane and numbered carbons refer to the structure in Scheme 1.

Carbon number	^{13}C-chemical shift (ppm)				
	Solution (CD_3CN)	Solid state		Shift difference [a]	
		I	II	I	II
1	143.69	143.4	145.5, 146.6	0.29	−1.81/ −2.91
2 or 3	108.63	105.0	105.3	3.63	3.33
3 or 2	111.57	109.7	111.0	1.87	0.57
4	137.85	140.8	140.8	−2.95	−2.95
5	40.64	36.3	39.8	4.34	0.84
6	152.35	149.6	150.5	2.75	1.85
7 or 10	114.72	116.6	–	−1.88	–
8	127.06	125.5	127.3	1.56	−0.24
9	154.29	152.6	152.5	1.69	1.79
10 or 7	135.07	134.6	133.6	0.47	1.47
11	109.16	108.3	108.6	0.86	0.56
12	169.14	171.3	171.2, 172.7	−2.16	−2.06/ −3.56

[a] The difference between solution–solid state chemical shift data.

lised frusemide samples was analysed by GLC. Samples of frusemide I and II were found to contain equivalent amounts of water (0.1–0.2% w/w water). The data suggest that it is not the total amount of water taken up by the crystals that is the critical factor in the formation of frusemide II. Moreover, the distribution of the water within the crystals or a specific drug–solvent interaction may be postulated to be the important factors.

TABLE 4

Proton relaxation data (T_1 and $T_{1\rho}$) for frusemide I and II in the solid state

Proton relaxation time	Frusemide I	Frusemide II
T_1 (s)	2.7	2.3
$T_{1\rho}$ (ms)	73	128 (80% population) 28 (20% population)

The results of the chemical analyses gave no indication of increased levels of impurity or water content in frusemide samples recrystallised as frusemide II. These data suggest that the observed solid state changes in the frusemide II crystal are unlikely to be a result of differing levels of trace impurity.

Equilibrium solubility

Equilibrium solubility measurements in pH 4.95 sodium acetate–acetic acid buffer (37 °C) revealed frusemide II (methanol recrystallisation) to have a significantly higher solubility (57.13 mg/100 ml) than the untreated frusemide sample (35.17 mg/100 ml). The addition of water (5–20% v/v) to the methanol solvent resulted in samples having solubilities equivalent to the original material (35.12–35.35 mg/100 ml). The higher aqueous solubility of frusemide II reflects an increased crystal energy originating from the alteration of the solid state characteristics of the material.

Frusemide is poorly soluble in acidic media and dissolution may therefore be solubility controlled. The demonstrated increased solubility for frusemide II may be relevant in vivo and consequently there is a pharmaceutical requirement to have a consistent and controlled crystal form.

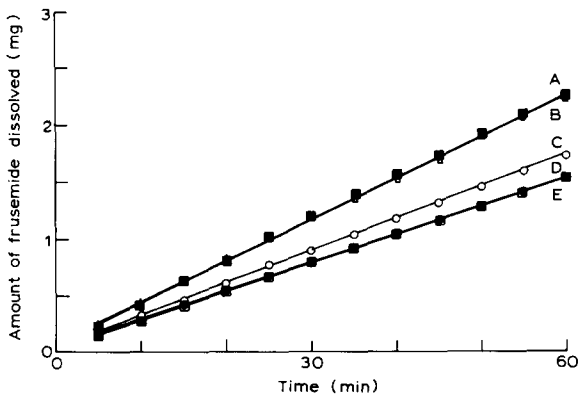

Fig. 6. Representative dissolution profiles from constant surface area discs in pH 4.95 acetate buffer at 37 °C for untreated frusemide and recrystallised frusemide samples; recrystallisation from ethanol (A) and methanol (B) harvested from the side of the evaporating dish, standard frusemide (C), methanol recrystallisation harvested from the bottom of the dish (D) and commercial frusemide sample (E).

Intrinsic dissolution

Using the constant surface area dissolution apparatus, samples of frusemide I and II were tested in pH 4.95 sodium acetate–acetic acid buffer at 37 °C. The data (Fig. 6) show frusemide II to exhibit a linear release profile and a significantly higher dissolution rate (38.6 $\mu g \cdot min^{-1}$) than the untreated frusemide (24.2 $\mu g \cdot min^{-1}$) or standard frusemide (27.3 $\mu g \cdot min^{-1}$) samples. The increased equilibrium solubility for frusemide II in the same medium readily explains the magnitude of the increased dissolution rate. Samples recrystallised from methanol in the presence of 5% v/v added water gave dissolution rates equivalent to the untreated material (25.7 $\mu g \cdot min^{-1}$), correlating well with equilibrium solubility data.

The demonstration of an increased aqueous equilibrium solubility and dissolution rate from constant surface area discs for frusemide II, in comparison to frusemide I, is consistent with the formation of an energetically dissimilar crystal form.

Conclusion

The solid state analyses of frusemide samples produced by the solvent evaporation process defined a second, novel, frusemide crystal form (frusemide II) from a methanol or ethanol recrystallisation of frusemide I. The formation of frusemide II was dependent upon specific conditions and solvent composition. The presence of water disrupted the formation of frusemide II from methanol and ethanol–water co-solvents.

Frusemide II was differentiated from frusemide I by DSC and XPD. In particular an endotherm present 81 °C below the melting endotherm of frusemide I was not found in the thermogram of frusemide II. A subtle change in molecular conformation and crystal packing has been proposed to account for the endothermic process. Differences in the hydrogen bonding sequence in each crystalline form were indicated by IR data. Solid state ^{13}C-NMR spectra for the two crystal forms revealed marked differences in the chemical shift and peak splitting characteristics reflecting a change in the molecular conformation. A two-component $T_{1\rho}$ relaxation profile for frusemide II indicated the presence of a more mobile element within a rigid phase while frusemide I, possessing only a single $T_{1\rho}$ relaxation time, was shown to be more uniformly ordered.

The physicochemical consequences of the change in the crystal form of frusemide I to frusemide II include a 63% increase in equilibrium solubility and a 58% increase in the dissolution rate measured from constant surface area discs (pH 4.95 buffer). In the case of frusemide, a sparingly water-soluble drug, these effects may produce significant bioavailability changes.

Acknowledgements

The authors would like to thank the SERC and Pfizer, U.K. (Dr. R. Davidson) for a CASE award for Dr. C. Doherty, Dr. D. Chenery (Mattson Instruments Ltd., UK) for help with the VT-FTIR spectra, Dr. M. Kinns (Pfizer, U.K.) for the ^{13}C-solution spectra, the solid state NMR group at the University of East Anglia (Mike Cudby) for solid state NMR data and the SERC for providing the necessary additional funding.

References

Bellows, J.C. and Chen, F.P., Determination of drug polymorphs by laser Raman spectroscopy I. Ampicillin and griseofulvin. *Drug Dev. Ind. Pharm.*, 3 (1977) 451–458.

Bolton, B.A. and Prasad, P.N., Laser Raman investigation of pharmaceutical solids: griseofulvin and its solvates. *J. Pharm. Sci.*, 70 (1981) 789–793.

Burger, A. and Ramberger, R., On the polymorphism of pharmaceuticals and other molecular crystals I. Theory and thermodynamic rules. *Mikrochemica Acta*, 11 (1979a) 259–271.

Burger, A. and Ramberger, R., On the polymorphism of pharmaceuticals and other molecular crystals II: Applicability of thermodynamic rules. *Mikrochemica Acta*, 11 (1979b) 273–316.

Burger, A. and Ramberger, R., Thermodynamics and IR spectroscopy of four polymorphs of pyrithyldione. *Mikrochemica Acta*, 1 (1981) 217–225.

Byrn, S.R., Gray, G., Pfeiffer, R.R. and Fyfe, J., Analysis of solid state NMR spectra of polymorphs (benoxaprofen and nabilone) and pseudopolymorphs (cefazolin). *J. Pharm. Sci.*, 74 (1985) 565–568.

Byrn, S.R., McKenzie, A.T., Hassan, M.M.A. and Al-Badr, A.A., Conformation of glyburide in the solid state and in solution. *J. Pharm. Sci.*, (1986) 596–600.

Carstensen, J.T., *Theory and Practice of Pharmaceutical systems II; Heterogeneous Systems*, Academic, London, 1973, pp. 14–19.

Christensen, S.A. *Synthesis of Frusemide.* West German Patent, No. 1,801,778, 1967.

Christensen, S.A. *Method for the Manufacture of N-Substituted Anthranilic Acid Derivatives.* British Patent, No. 1,256,774, 1969.

Chrzanowski, F.A., Fegely, B.J., Sisco, W.R. and Newton, M.P., Analysis of *N*-(4-hydroxyphenyl) retinamide polymorphic forms by X-ray diffraction. *J. Pharm. Sci.*, 73 (1984) 1448–1450.

Clark, E.G.C., *Isolation and Identification of Drugs*, Pharmaceutical Press, London, 1969, p. 741.

DeCamp, W.H., X-Ray diffraction data for selected drugs: frusemide, hydrochlorothiazide, naproxen, naproxen sodium, propranolol hydrochloride and the halopheniramine maleates. *J. Ass. Off. Anal. Chem.*, 67 (1984) 927–933.

Doherty, C. and York, P., Mechanism of dissolution of frusemide–PVP solid dispersions. *Int. J. Pharm.*, 34 (1987a) 197–205.

Doherty, C. and York, P., Evidence for solid and liquid state interactions in a furosemide–polyvinylpyrrolidone solid dispersion. *J. Pharm. Sci.*, 76 (1987b) 731–737.

Doi, M., Yasuda, N., Ishida, T. and Inoue, M., Physicochemical studies of medicinal drug polymorphism I. Structural studies of bromodiethylacetylurea by thermal and X-ray crystal analysis. *Chem. Pharm. Bull.*, 33 (1985) 2183–2189.

Dupont, L., Frusemide Infrared Spectrum in Personal Communication from the University of Leige, Belgium, 1985.

Flippen-Anderson, J.L., Gilardi, R., Karle, I.L., Frey, M.H., Opella, S.J., Gierasch, L.M., Goodman, M., Madison, V. and DeLaney, N.G., Crystal structures, molecular conformations, infrared spectra and ^{13}C-NMR spectra of methyl-proline peptides in the solid state. *J. Am. Chem. Soc.*, 105 (1983) 6609–6614.

Fyfe, C., *Solid State NMR for Chemists*, CFC Press, Guelph, Canada, 1983, p. 324.

Haleblian, J. and McCrone, W., Pharmaceutical Applications of Polymorphism. *J. Pharm. Sci.*, 58 (1969) 911–929.

Havens, J.R. and Koenig, J.L., Applications of high resolution ^{13}C-NMR to solid polymers. *Appl. Spec.*, 37 (1983) 226–249.

Kenwright, A.M., PhD thesis, University of East Anglia, 1986.

Lamotte, J., Campsteyn, H., Dupont, L. and Vermeire, M., Structure cristalline et moleculaire de l'acide furfurylamino-2-chloro-4 sulfamoyl-5-benzoique, la furosemide ($C_{12}H_{11}ClN_2O_5S$). *Acta Cryst.*, B34 (1978) 1657–1661.

Miyata, T., Nakagawa, H., Akimoto, K., Sugimoto, I., Marti, E. and Heiber, O., Crystal forms of cianidanol. *Yakugaku Zasshi*, 105 (1985) 59–64.

Pouchert, C.J., *The Aldrich Library of Infrared Spectra*, Aldrich Chemical Co., 1970.

Ripmeester, J.A., Application of solid state ^{13}C-NMR to the study of polymorphs, clathrates and complexes. *Chem. Phys. Lett.*, 74 (1980) 536–538.

Sekiguchi, K., Shirotani, K., Yuasa, H., Suzuki, E. and Nakagawa, F., Size reducability of sulphathiazole by heat transition and subsequent ball milling. *Chem. Pharm. Bull.*, 28 (1980) 3203–3209.

Shin, S.C., Studies on hydrophobic drug-soluble carrier coprecipitates II: Physicochemical characteristics of furosemide–PVP coprecipitates. *Arch. Pharm. Res.*, 2 (1979) 49–64.

Yellin, H., Konfino, E. and Gan, R., *Process for the preparation of 4-chloro-N-furfuryl-5-sulfamoylanthranilic acid.* United States Patent, No. 3,780,067, 1973.

York, P., Solid state properties of powders in the formulation and processing of solid dosage forms. *Int. J. Pharm.*, 14 (1983) 1–28.